

Magnetic Properties at Surface Boundary of a Half-Metallic Ferromagnet $\text{La}_{0.7}\text{Sr}_{0.3}\text{MnO}_3$

J.-H. Park,¹ E. Vescovo,¹ H.-J. Kim,¹ C. Kwon,^{2,*} R. Ramesh,² and T. Venkatesan²

¹National Synchrotron Light Source, Brookhaven National Laboratory, Upton, New York 11973-5000

²Center for Superconductivity Research, Department of Physics, University of Maryland, College Park, Maryland 20742

(Received 2 March 1998)

The surface-boundary magnetization (M_{SB}) for a manganese perovskite $\text{La}_{0.7}\text{Sr}_{0.3}\text{MnO}_3$ has been investigated using spin-resolved photoemission spectroscopy, which has an ~ 5 Å probing depth. M_{SB} shows the full moment at very low temperature but decays much faster than the bulk magnetization (M_B) upon heating. This result provides direct insight into various novel properties at grain and surface boundaries observed in the polycrystalline samples and junctions of manganese perovskites. [S0031-9007(98)06948-8]

PACS numbers: 75.30.Pd, 78.70.Dm, 79.60.Bm

Since the discovery of the large negative magnetoresistance (MR) in doped manganese perovskites [1–3], these compounds have attracted much interest, especially due to their potential technological applications. However, the large MR response requires magnetic fields as high as several tesla, which are only available in special environments. Recently, enhanced low-field MR effects have been reported in the polycrystalline samples [4,5] and trilayer tunnel junctions in which a thin insulating layer is sandwiched by the ferromagnetic metallic manganese perovskite layers [6,7]. In spite of their completely different forms, the origin of the low-field MR has been interpreted by the same spin-dependent tunneling mechanism; in the case of polycrystalline samples across the grain boundary [8] and in the trilayer devices through the insulating layer. The spin-dependent tunneling is induced by the spin anisotropy of the conduction electrons, and thus the low-field MR is expected to be directly related to the magnetization of the ferromagnetic metals. Despite this fact, the reported low-field MR for the manganese perovskites decreases rapidly with an increase of temperature, exhibiting the temperature dependence which is inconsistent with that of the magnetization, and is different from that for the pyrochlore manganite, $\text{Tl}_2\text{Mn}_2\text{O}_7$, which shows a temperature dependence proportional to the cube of the magnetization [9].

Tunneling is a mechanism that occurs at the surface (grain/interface) boundary, and the tunneling conductivity is dominated by charge carriers at the surface boundary. Thus, the anomalous physical behavior in polycrystalline samples or junction devices has often been attributed to extrinsic factors such as defects or stoichiometry at the surface (grain/interface) boundaries. In fact, many complex oxides including high T_c superconducting cuprates are well known to easily form defects or variations in stoichiometry at surface boundaries. However, it is also suspected that in the manganese perovskites the magnetization behaves quite differently at the surface than in the bulk due to the lower effective magnetic interactions caused by the surface termination of the crystal structure [9].

Earlier theoretical studies using the mean field approximation and numerical Monte Carlo simulations based on the semi-infinite Heisenberg model predicted that the temperature dependence of the surface magnetization characterized by $\beta = 1$ and $\beta \approx 0.8$ in $(T_c - T)^\beta$ near T_c differs greatly from the temperature dependence of $\beta = \frac{1}{2}$ and $\beta \approx \frac{1}{3}$ predicted for the bulk magnetization, respectively [10,11]. In a few ferromagnetic simple metals such as nickel, iron, and gadolinium, the magnetization was reported to show a different temperature dependence at the surface compared with the bulk [12–14]. Therefore, clarifying the magnetization at the surface boundary of the manganese perovskite is essential to the understanding of the low-field MR induced by the spin-dependent tunneling mechanism, which also contributes to pair breaking in superconducting cuprate/ferromagnetic manganite heterostructure devices [15,16].

In this Letter, we present the temperature dependence of the magnetization at the surface boundary (M_{SB}) obtained using spin-resolved photoemission spectroscopy (SPES), which has an ~ 5 Å probing depth. M_{SB} exhibits greatly different temperature dependence than that of the bulk magnetization (M_B). Magnetization with another length scale was also determined from the Mn L -edge absorption magnetic circular dichroism (MCD) with an ~ 50 Å of the probing depth. Finally, we found that the polarized charge carrier density at the surface boundary shows a temperature dependence similar to that of the low-field MR for the polycrystalline samples.

A 1900 Å thick $\text{La}_{0.7}\text{Sr}_{0.3}\text{MnO}_3$ ($T_c \approx 360$ K) epitaxial thin film was deposited on a (001) SrTiO_3 substrate by conventional pulse laser deposition [17]. As shown in Fig. 1, the magnetization of the film measured with a superconducting quantum interference device (SQUID) shows the temperature dependence which is very similar to that for a bulk crystal sample [4,18,19]. However, the magnetic domain properties of the thin film are enormously improved, possibly due to surface stress and finite-size effects. The bulk crystals typically require fields of several tesla to saturate the magnetization and

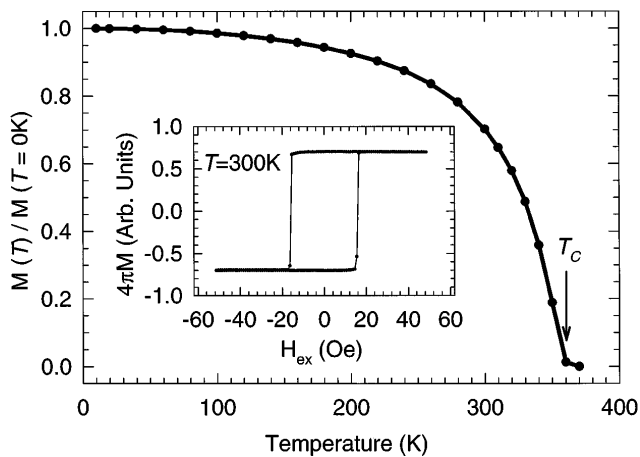


FIG. 1. Temperature dependence of magnetization measured by SQUID at 200 Oe. The inset shows the magnetization (M) vs applied magnetic field (H) hysteresis loop, which was obtained by the magneto-optical Kerr effect (MOKE).

yield very little remanent magnetization. However, as shown in the inset of the figure, the thin film shows a single-domain-type magnetic hysteresis, i.e., $\sim 100\%$ remanent magnetization and very low coercive field (~ 20 Oe at 300 K and ~ 100 Oe at 40 K).

SPES measurements were performed at the new U5UA undulator beam line at the National Synchrotron Light Source (NSLS) at Brookhaven National Laboratory [20]. An ~ 200 Oe magnetic pulse field was used for the magnetization. The base pressure was better than 1×10^{-10} Torr. The sample was introduced to the ultra-high vacuum chamber, and the surface was then cleaned *in situ* in a sequence of annealing processes, which will be presented in detail elsewhere. The successful achievement of a clean surface is confirmed by the observation of the metal-nonmetal transition in the photoemission study across T_c and of the half-metallic nature in SPES measurements well below T_c [21]. Considering that SPES measurements are performed at zero-magnetic field by using the remanent magnetization, even the single-magnetic-domain property is conserved at the surface. The spectrum does not display any noticeable angular dependence, indicating that the surface normal is completely obscured by the rough surface (~ 20 Å roughness), and the obtained whole valence band spectrum is very identical to the angle-integrated one [22]. MCD x-ray absorption spectroscopy (XAS) measurements were performed at the renewed U4B beam line also at NSLS. The photon beam was set with $\sim 85\%$ helicity with 0.3 eV energy resolution. The incident beam was 45° off from the surface normal.

Figure 2 shows the temperature dependent spin anisotropy obtained by SPES measurements on the $\text{La}_{0.7}\text{Sr}_{0.3}\text{MnO}_3$ film. The inset shows SPES spectra measured at $T = 40$ K. The spectra clearly manifest the *half-metallic* feature, i.e., the metallic Fermi cutoff for the majority spin with the disappearance of the spectral

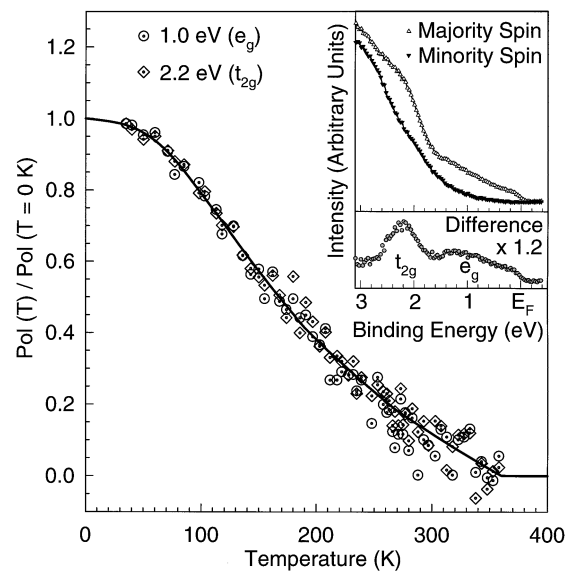


FIG. 2. Temperature dependence of spin polarization of Mn $3d$ states, e_g at 1.0 eV binding energy and t_{2g} at 2.2 eV binding energy obtained with $h\nu = 40$ eV. The inset shows the spin-polarized photoemission spectra for the majority and minority spins and the difference at 40 K as presented in Ref. [21].

weight very near E_F —reflecting the insulating gap—for the minority spin [21]. The difference spectrum shows Mn $3d$ states which split into t_{2g} and e_g states due to the octahedral crystal field as indicated in the figure. For both states, the temperature dependence of the spin anisotropy, which was monitored separately, shows nearly identical behavior, confirming that the spin anisotropy represents the magnetization. The photoelectron has a few monolayers (~ 5 Å) penetration depth, and thus the spin anisotropy corresponds to M_{SB} . Interestingly, M_{SB} shows a greatly different temperature dependence than M_B in Fig. 1. It shows nearly the full moment at low temperature ($T < \sim 60$ K), and then decreases gradually upon heating up to T_c . M_{SB} shows a linearlike temperature dependence near T_c , but considering the large experimental uncertainty, the determination of the power law seems to be somewhat beyond the experimental capability. The anisotropy disappears above T_c , showing that the T_c at the surface boundary is very close to that of the film as a whole. In the manganese perovskites, T_c varies with the oxygen content, and thus the deviation of the oxygen stoichiometry at the surface boundary appears to be negligible.

Figure 3 shows XAS spectra at Mn $L_{2,3}$ edge for different helicities relative to the magnetization and the MCD spectrum of $\text{La}_{0.7}\text{Sr}_{0.3}\text{MnO}_3$ measured at 40 K. The spectra were recorded by monitoring the sample current, which corresponds to the total electron yield, and an ~ 200 Oe pulse field along the in-plane easy axis was used for the magnetization of the sample. The spectra for the two different helicities were recorded by alternating the magnetization at every photon energy in order

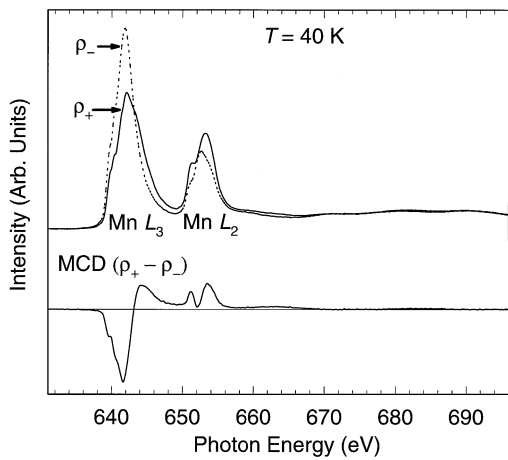


FIG. 3. X-ray absorption and the magnetic circular dichroism (MCD) spectra at Mn L -edge. ρ^+ and ρ^- denote the absorption spectra for the photon helicity parallel and antiparallel to the magnetization, respectively. The photon incident angle and the degree of the circular polarization were taken into account for the spectra.

to minimize any possible artifacts. The XAS and MCD spectra are very similar to previous MCD results obtained from $\text{La}_{1-x}\text{Ca}_x\text{MnO}_3$ [23] and $\text{La}_{1-x}\text{Sr}_x\text{MnO}_3$ bulk samples [24]. The MCD anisotropy, the difference divided by the sum of the two absorption signals, is as high as $\sim 23\%$, reflecting large magnetic moments at Mn. The MCD spectrum displays a complicated multiplet structure, which can be understood by theoretical multiplet calculations. Here we will focus on the temperature dependence of the MCD anisotropy, which is proportional to the magnetization. Upon heating, the anisotropy decreases without any considerable change in the line shape.

XAS in the total electron yield mode has ~ 50 Å probing depth, which corresponds to an intermediate length scale between the bulk and the surface boundary. Hence, the MCD anisotropy corresponds to an intermediate length scale magnetization (M_{IM}). Figure 4 shows the temperature dependence of the magnetization for three different length scales. M_{IM} exhibits a temperature dependence which is closer to that of M_B compared with that of M_{SB} , but its deviation from M_B is still significant. The deviation could be due to the contribution from the surface boundary. However, the contribution of the first ~ 5 Å surface boundary to the XAS is at most $\sim 10\%$, and thus the observed large deviation indicates that for at least several monolayers below the surface boundary the magnetization is considerably different from M_B .

Previous photoemission studies of the manganese perovskites showed that the density of states (DOS) at the Fermi energy (E_F) increases upon cooling below T_c [22,25]. In order to investigate the temperature dependence of the charge carriers at the surface boundary, we have performed a temperature dependent study by monitoring the photoemission spectral weight at 0.1 eV binding energy which is indicated in the near- E_F

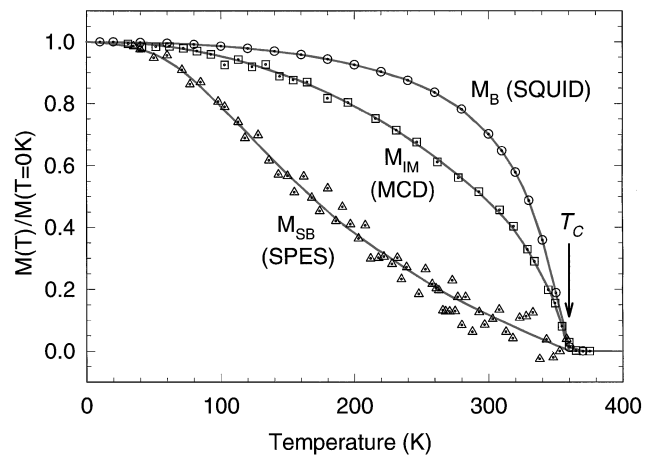


FIG. 4. Summarized temperature dependence of magnetization for different length scales. M_B , M_{IM} , and M_{SB} denote the bulk, the intermediate length scale (~ 50 Å), and the surface boundary (~ 5 Å) magnetization, which were determined by SQUID, soft x-ray MCD, and SPES, respectively. The M_{SB} data points represent the average values of the spin anisotropy of the e_g and t_{2g} states in Fig. 2.

photoemission spectra presented in the inset of the figure. The spectral weight at 0.1 eV binding energy does not truly account for $\text{DOS}(E_F)$, but, considering the technical difficulties arising from the finite experimental resolution (0.1 eV full width half maximum) and the Fermi-Dirac occupation function, it seems to be the best choice. Figure 5 shows the temperature dependence. As can be seen in the inset, the spectrum displays considerable spectral weight at 0.1 eV binding energy together with the metallic Fermi cutoff at very low temperature.

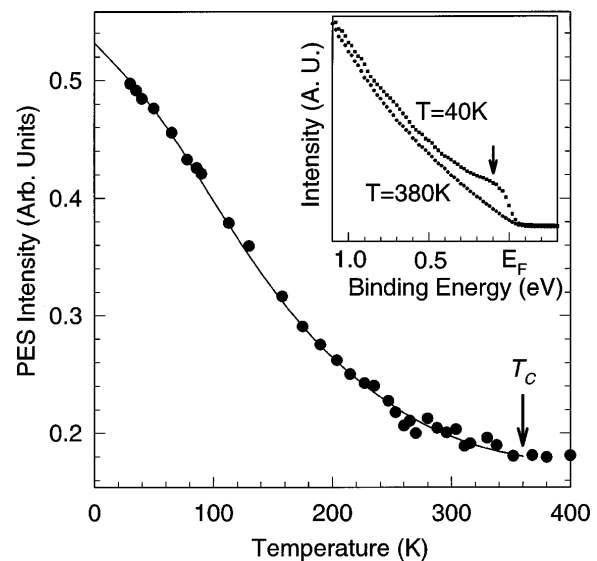


FIG. 5. Temperature dependence of the photoemission spectral weight at 0.1 eV binding energy obtained with $h\nu = 40$ eV. The 0.1 eV binding energy is indicated by an arrow in the inset, which shows the near- E_F photoemission spectra above (380 K) and well below (40 K) the Curie temperature ($T_c \approx 360$ K), as presented in Ref. [21].

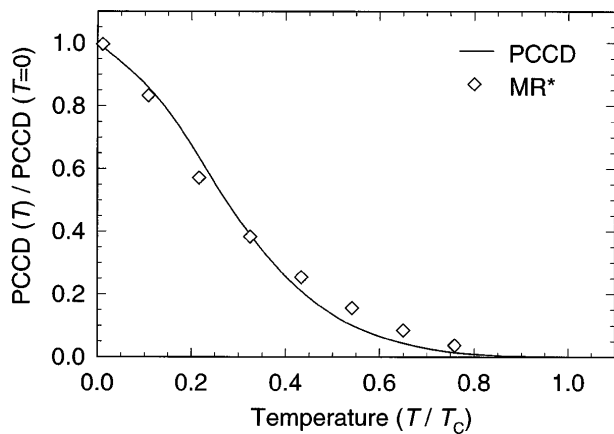


FIG. 6. Temperature dependence of polarized charge carrier density (PCCD) at the surface boundary comparison with that of the low-field magnetoresistance (MR^*) quoted from Ref. [4]. The PCCD and MR^* are scaled by their extrapolated values for $T = 0$ K.

Upon heating, the spectral weight continuously decreases up to T_c , and then stays nearly constant. As expected from the 380 K spectrum in the inset, this quantity becomes smaller when the binding energy approaches E_F . If the experimental resolution is taken into account, $DOS(E_F)$ is expected to be negligible above T_c . Previous studies of a $La_{0.825}Sr_{0.175}MnO_3$ single crystal using optical absorption, which is a bulk sensitive technique, show that $DOS(E_F)$ estimated from the Drude weight decreases linear-likely upon heating up to T_c [18]. Even considering all the existing uncertainties, it is clear that $DOS(E_F)$ at the surface boundary deviates significantly from that of the bulk, as expected from the large difference between M_{SB} and M_B .

In most other ferromagnetic metals, $DOS(E_F)$ has very little variation with temperature, and the polarized charge carrier density (PCCD), which is the difference in the charge carrier densities for the different spins, is very closely proportional to the magnetization (M). However, in the manganese perovskites, $DOS(E_F)$ varies strongly with temperature below T_c . Thus PCCD does not agree with M , and PCCD is represented by $DOS(E_F) \times M$. Figure 6 shows the temperature dependence of PCCD at the surface boundary of $La_{0.7}Sr_{0.3}MnO_3$ ($T_c \approx 360$ K) in comparison with that of the low-field MR^* , which is defined as $\Delta\rho(H)/\rho(H=0)$, of a polycrystalline $La_{0.67}Sr_{0.33}MnO_3$ ($T_c \approx 365$ K) sample [4]. Here, PCCD is estimated with the assumption that $DOS(E_F)$ becomes zero above T_c . The temperature is scaled by the T_c in order to account for the differences in T_c . The obtained PCCD shows a similar temperature dependence to that of the low-field MR^* . In fact, the transport properties of the manganese perovskites are strongly affected by various complex mechanisms such as strong-polaron formation, Jahn-Teller distortion, and charge and orbital ordering, and thus PCCD cannot be simply related to the low-field MR^* . However, this result indicates that the low-

field MR^* of the manganese perovskites, which is induced by the spin-dependent intergrain transport mechanism, is intimately related to PCCD at the surface boundary.

In conclusion, we have presented details of the magnetic properties at the surface boundary of a half-metallic ferromagnet, $La_{0.7}Sr_{0.3}MnO_3$. We found that the magnetism at the surface boundary is significantly different from that of the bulk. The results obtained provide critical information on the understanding of the novel properties at the surface boundaries of the manganese perovskite.

We thank J.B. Hastings and S.L. Hulbert for helpful discussions. NSLS is supported by the Department of Energy under Contract No. DE-AC02-76CH00016, and the work in UM is partially supported by the NSF-MRSCC under Grant No. DMR96-32521.

*Present address: Superconductivity Technology Center, Los Alamos National Laboratory, Los Alamos, NM 87545.

- [1] R. von Helmholt *et al.*, Phys. Rev. Lett. **71**, 2331 (1993).
- [2] K. Charhara *et al.*, Appl. Phys. Lett. **63**, 1990 (1993).
- [3] S. Jin *et al.*, Science **264**, 413 (1994).
- [4] H. Y. Hwang, S-W. Cheong, N.P. Ong, and B. Batlogg, Phys. Rev. Lett. **77**, 2041 (1996).
- [5] A. Gupta *et al.*, Phys. Rev. B **54**, R15 629 (1996).
- [6] Y. Lu *et al.*, Phys. Rev. B **54**, R8357 (1996).
- [7] J. Z. Sun *et al.*, Appl. Phys. Lett. **70**, 1769 (1997).
- [8] It has also been discussed that the intergrain tunneling in the polycrystalline samples is distinguishable from the "ordinary" tunneling mechanism which is supposed to be across an insulating barrier [X.W. Li, A. Gupta, Gang Xiao, and G.Q. Gong, Appl. Phys. Lett. **71**, 1124 (1997)].
- [9] H. Y. Hwang and S-W. Cheong, Nature (London) **389**, 943 (1997).
- [10] K. Binder, in *Phase Transitions and Critical Behavior*, edited by C. Domb and J.L. Lebowitz (Academic Press, London, 1983), Vol. 8, pp. 1-144.
- [11] K. Binder and P.C. Hohenberg, Phys. Rev. B **9**, 2194 (1974).
- [12] E. Kisker, K. Schröder, W. Gudat, and M. Campagna, Phys. Rev. B **31**, 329 (1985).
- [13] S.F. Alvarado, M. Campagna, and H. Hopster, Phys. Rev. Lett. **48**, 51 (1982).
- [14] C. Rau, J. Magn. Magn. Mater. **30**, 141 (1982).
- [15] V. A. Vas'ko *et al.*, Phys. Rev. Lett. **78**, 1134 (1997).
- [16] Z. W. Dong *et al.*, Appl. Phys. Lett. **71**, 1718 (1997).
- [17] C. Kwon *et al.*, J. Magn. Magn. Mater. **172**, 229 (1997).
- [18] Y. Okimoto *et al.*, Phys. Rev. Lett. **75**, 109 (1995).
- [19] Z. Trajanovic *et al.*, Appl. Phys. Lett. **69**, 1005 (1996).
- [20] E. Vescovo *et al.*, National Synchrotron Light Source Activity Report 1996 No. BNL-52517, A-25; J. Unguris, D. T. Pierce, and R. J. Celotta, Rev. Sci. Instrum. **57**, 1314 (1986).
- [21] J.-H. Park *et al.*, Nature (London) **392**, 794 (1998).
- [22] D. D. Sarma *et al.*, Phys. Rev. B **53**, 6873 (1996).
- [23] J.-H. Park *et al.*, J. Appl. Phys. **79**, 4558 (1996).
- [24] E. Pellegrine *et al.*, National Synchrotron Light Source Activity Report 1996 No. BNL-52517, A-20.
- [25] J.-H. Park *et al.*, Phys. Rev. Lett. **76**, 4215 (1996).